Residual Crush Energy Partitioning, Normal and Tangential Energy Losses 07B-34

Raymond M. Brach
Brach Engineering, LLC
University of Notre Dame
rbrach@nd.edu

Kevin J. Welsh
Struble-Welsh Engineering, Inc.
kwelsh@strublewelsh.com

R. Matthew Brach
Brach Engineering, LLC
matt_brach@brachengineering.com

Abstract: Residual damage caused during a collision has been related through the use of crush energy models and impact mechanics directly to the collision energy loss and vehicle velocity changes, ΔV_1 and ΔV_2. The simplest and most popular form of this crush energy relationship is a linear one and has been exploited for the purpose of accident reconstruction in the well known CRASH3 crush energy algorithm. Nonlinear forms of the relationship between residual crush and collision energy also have been developed. Speed reconstruction models that use the CRASH3 algorithm use point mass impact mechanics, a concept of equivalent mass, visual estimation of the Principle Direction of Force (PDOF) and a tangential correction factor to relate total crush energy to the collision ΔV values. Most algorithms also are based on an assumption of a common velocity at the contact area between the vehicles. The use of point mass mechanics, equivalent mass, a tangential correction factor and zero restitution are unnecessarily restrictive and their use reduces the accuracy of the crush energy methods in crash reconstruction.

This paper shows that planar impact mechanics can be adapted to significantly improve the rigor of using residual crush for crash reconstruction. Planar impact mechanics models the impulses and the changes in momentum of vehicles colliding in a plane including restitution of the collision at the intervehicular contact surface. Two impact coefficients are used, the (normal) coefficient of restitution and the (tangential) impulse ratio. The work of the normal component and tangential component of the crash impulse vector are individually associated with the crush energy and with the tangential energy loss and to each vehicle's ΔV. This work-energy association is referred to as partitioning of the collision energy loss. Partitioning is necessary in order to adapt planar impact mechanics to the CRASH3 measurement protocol. The paper also covers the proper approach to take restitution into account, both as it occurs in the barrier tests to determine each vehicle's crush stiffness coefficients and as it occurs in the impact between two vehicles. Data from oblique frontal barrier crash tests by Struble-Welsh Engineering are used to assess the use of planar impact mechanics and the partitioning of energy loss into crush energy and tangential energy. The process of using crush energy in reconstructions is discussed.

INTRODUCTION

CRASH3 (Calspan Reconstruction of Accident Speeds on the Highway) is an acronym used frequently in the field of accident reconstruction and represents a method for reconstructing the initial speeds of a pair of colliding vehicles based on their postimpact travel (distance from impact positions to their rest positions) and measurements of their residual crush. The CRASH3 method contains the following steps:

- vehicles' postimpact speeds (speeds at separation) are estimated using the postimpact travel using an approximate method developed by Marquardt,
- the energy expended in the collision, E_C, is estimated using a method developed by Campbell and modified by Prasad (called here the crush energy algorithm),
- using point mass impact mechanics to calculate each vehicles' ΔV, CRASH3 combines the postimpact speeds and the crush energy to estimate the preimpact speeds. The analytical foundation used for the calculation of ΔV by CRASH3 contains several simplifying assumptions, including:

1. the use of common velocity conditions,
2. point mass impact dynamics and equivalent mass,
3. energy correction factor for tangential contact effects.

This paper discusses and presents the use of planar impact mechanics [1] to provide a more rigorous and accurate approach to combine the crush energy algorithm to the speed changes of the vehicles. It relaxes the above three assumptions (see Appendix A). The proposed approach is as follows:

- Crush energy from the CRASH3 crush energy algorithm is equated to the work of the normal component of the contact impulse from planar impact mechanics.
- The work of the tangential component of planar impact mechanics is used in place of the CRASH3 tangential correction factor.
- Each vehicle's ΔV is calculated with the appropriate value of the coefficient of restitution and impulse ratio using planar impact mechanics.

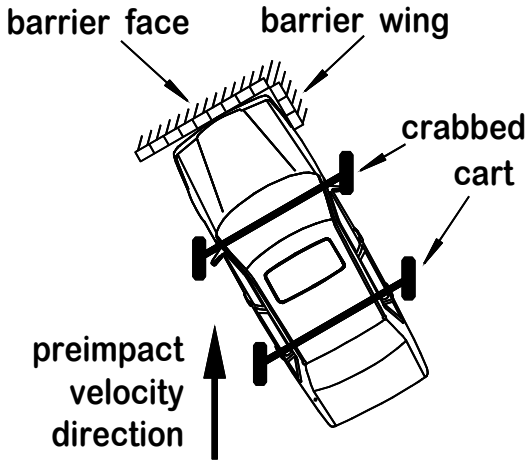

Figure 1. Test configuration.

The paper also compares some recent test results [2] to illustrate the details of this approach. Comparisons show good agreement with theory.

Three sequential crabbed crash tests [2] of a single 2002 Chevrolet Cavalier were carried out at speeds of 13.11, 23.12 and 29.02 mph into a winged rigid barrier [2]; see Figure 1. In addition to the normal frontal crush, the crabbed orientation and barrier wing induced significant tangential deformation and also constrained the final tangential motion to be zero along the main barrier face. Comparisons are made of the ability of planar impact mechanics to model the barrier impacts and of a combination of the CRASH3 crush analysis and planar impact mechanics to properly partition the collision energy loss. A particular comparison is made of the critical impulse ratio values from planar impact mechanics with the test values.

PLANAR IMPACT MECHANICS

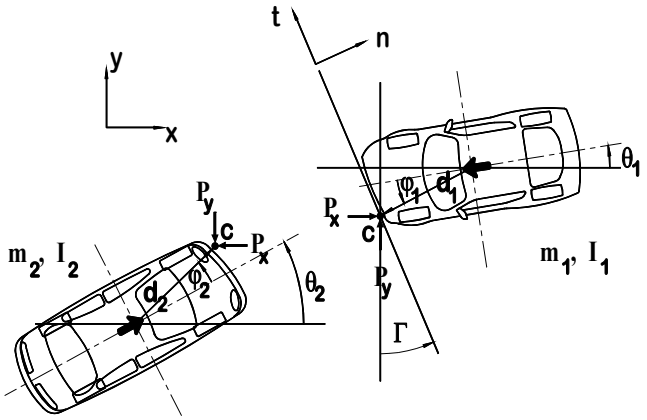

Figure 2. Free body diagrams and coordinates of impacting vehicles.

The use of impact mechanics, in one form or another, to model the collision of two vehicles has been studied and used for many years [3,4,5,6]. Only a summary of some of the main points is included here. For a detailed discussion, see [7]. The use of the work of impulses associated with planar impact mechanics [1] is a relatively more recent feature and allows a more rigorous approach to partitioning the energy dissipated in a collision and its association with the CRASH3 crush energy algorithm. Additional treatment of this is included here.

Figure 2 shows free body diagrams of two colliding vehicles. The *x-y* axes are fixed to the ground. The relative orientation of the *n-t* axes is through the angle Γ. Following the usual assumptions [7] for the use of impulse and momentum and from Newton's laws, the equations for the changes in the velocity components can be written in closed form and are given in Appendix A. Note that this problem is posed and solved as an initial value problem, that is, the initial velocities are known and the final velocities are calculated. Two of the important results of the solution of the planar impact equations are the expressions for the collision energy loss and for the ΔV of each vehicle. If kinetic energy is given the symbol T, the energy loss is T_L and the velocity changes of vehicles 1 and 2 are given in Eq 1 and Eq 2. All of the variables that appear in these equations are known and are defined in Appendix A.

Note that two impact coefficients, the coefficient of restitution, *e*, and the impulse ratio, μ, are part of the planar impact mechanics model [7]. The definitions of both *e* and μ are given in Appendix A. The coefficient of restitution, *e*, is associated with the normal (perpendicular) contact process over the intervehicular surface and μ is associated with the tangential contact process over the intervehicular surface. They are defined in the equation in Appendix A. The main topic of this paper is the establishment of the proper relationship of the crush energy, E_C, to the collision energy loss, T_L. To do this, it is necessary to examine the crush energy in more detail. According to Prasad [8], in its simplest form, crush energy, E^*, is related to residual crush by Eq 3.

$$T_L = \frac{1}{2}\bar{m}qv_{rn}^2(1+e)\left[2+2\mu r-(1+e)q\left(1+\mu^2+\frac{\bar{m}d_e^2}{m_1k_1^2}+\frac{\bar{m}d_f^2}{m_2k_2^2}\right)\right] \quad (1)$$

$$m_i\Delta V_i = \sqrt{\frac{2\bar{m}(1+e)q(1+\mu^2)T_L}{2+2\mu r-(1+e)q\left(1+\mu^2+\frac{\bar{m}d_e^2}{m_1k_1^2}+\frac{\bar{m}d_f^2}{m_2k_2^2}\right)}},\ i=1,2 \quad (2)$$

$$E^* = \sqrt{\frac{2E_C}{w}} = d_0 + d_1C \quad (3)$$

where d_0 and d_1 are experimentally determined crush stiffness coefficients, *w* is the width (extent) of the crush on the vehicle and *C* is the (average) depth of the residual crush. In practice, crush is measured according to a protocol [9] at *n* locations, typically *n* = 6, and is calculated using:

$$E_C = d_0^2K_1 + d_0d_1K_2 + d_1^2K_3 \quad (4)$$

where each K_i is a function of the *n* residual crush measurements, C_i [8]. According to the original development [10,11] and measurement protocol [9] each measurement of C_i is taken normal to the heading or transverse axes of the vehicle. This implies that the crush energy, E_C, is the energy expended by the deformation process normal (perpendicular) to the vehicle's undeformed, as manufactured, surface. In oblique collisions, energy also is expended during the tangential contact process. The work of any tangential effects (sliding, entanglement, deformation, etc.) must therefore be accounted for separately. Analytically, crush and crush energy is controlled by the normal impact coefficient, *e*, and the tangential work is controlled by the tangential impact parameter, μ.

The constants d_0 and d_1 depend on the specific vehicle and the location on the vehicle (front, rear, side) of the crush. Modifications [12,13] to the original crush model of Campbell have been made that incorporate restitution into the crush algorithm. However, the most direct way is to use the barrier test coefficient of restitution to determine the correct value of barrier crush energy to calculate the appropriate values of d_0 and d_1 for each vehicle and then to use the appropriate value of *e* corresponding to the collision restitution. In addition to the collision value of *e*, the collision value of μ must be known. For all collisions other than sideswipes, the impulse ratio takes on its critical value [7], μ_0,(see Appendix A). Recall that the critical impulse ratio, $\mu = \mu_0$ corresponds to the condition that the final relative tangential velocity at the impact center is zero, that is, sliding at the intervehicular surface ends at or before separation. Therefore, the simplest and most straightforward way to properly incorporate restitution into crush energy analysis is to use the proper individual vehicle barrier test values of *e* and the proper value of *e* for the vehicle-to-vehicle collision. Finally, it is important to note that the critical value of μ is dependent on the initial conditions (initial velocities) and the collision configuration.

Work of Normal and Tangential Impulses: The appropriate manner to apportion T_L once E_C is known and is now discussed. This section presents the background of the reconstruction method of using E_C with planar impact mechanics to reconstruct vehicle speeds. It also provides some insight into the sources and magnitudes of the uncertainties and some guidelines for the use of the method. Earlier work on the topic addressed the application of partitioning the work done

by the normal and tangential impulses in relation to the energy loss in a collision [1]. At the center of this reconstruction method is the need for a relationship between the work done by the normal and tangential impulses and the energy loss in a collision. Energy is not a vector whereas the intervehicular impulse is a vector quantity. However, for purposes of analyzing vehicular accidents, the energy associated with the residual deformation of a vehicle can be related to the work of the normal and tangential impulses generated while the vehicles are in contact and energy is lost due to the deformation of the vehicle components.

Consider, for example, the normal impulse, P_n. It is an internal action of the collision acting on the contact surface but is an external action to each vehicle. The work of P_n on each vehicle can be viewed as the energy loss associated with the residual normal crush deformation of that vehicle. The work of the tangential impulse, due to the forces developed from sliding, shearing plastic deformation and entanglement of vehicle components, can be viewed as the energy loss associated with the tangential contact effects.

In order for this work-energy relationship to be useful in the reconstruction of collisions involving automobiles, an expression that relates the work done by an impulse to the variables that are part of the planar impact mechanics model is needed. A relationship for computing the work of an impulse is given by a theorem [15] that states that the work done by any impulse, P, is given by the product of the magnitude of the impulse and the average velocity of the point of application of the impulse in the direction of the impulse. This relationship is expressed mathematically by:

$$W_P = \frac{1}{2}P(V+v) = P\frac{V+v}{2} \tag{5}$$

where v is the initial velocity and V is the final velocity of the point of application of the impulse P in the direction of the impulse. It is intuitive that the intervehicular contact forces do not act at a singular point during the time that the vehicles are in contact. However, the development of current planar impact mechanics models require that the impulse of the forces act at a point on the contact surface. This point, referred to as the *center of impact*, represents the spatial and temporal average (over the contact duration) for the location of the application of the impulses P_n and P_t during contact between the two bodies. Determination of the location of the impulse center in the application of this model requires judgement by the reconstructionist. The center of impact is labeled C in Figure 2.

Application of the relationship given by Eq 5 to the normal and tangential impulses generated during the impact between two rigid bodies requires that expressions for the initial and final velocities in the normal and tangential directions at the point of application of the impulses be written. For two rigid bodies the expressions for the initial and final relative velocities at the impact center in the normal direction are (v_{2Cn} - v_{1Cn}) and (V_{2Cn} - V_{1Cn}), respectively. Similar expressions for the tangential direction can be written by changing the n-subscript to a t-subscript. Introducing these expressions into Eq 5, writing the impulse using its normal and tangential components and grouping the terms into the normal and tangential components gives Eq 6. Since the impulse component, P_n, is normal to the intervehicular crush and residual crush is measured normal to the as-manufactured vehicle surface [9], the first work-energy term in Eq 6 has been associated with the residual crush and crush energy, E_C [1, 14]. Similarly, the second term has been associated with the tangential energy loss, E_T. In effect, this partitions the collision energy loss into two parts since from conservation of energy, $W_P = -T_L$. Consequently, E_C and E_T are given by Eq 7 and Eq 8, respectively.

$$W_P = \frac{1}{2}P_n[(v_{1Cn} - v_{2Cn}) + (V_{1Cn} - V_{2Cn})] + \frac{1}{2}P_t[(v_{1Ct} - v_{2Ct}) + (V_{1Ct} - V_{2Ct})] \tag{6}$$

$$E_C = \frac{1}{2}P_n[(v_{1Cn} - v_{2Cn}) + (V_{1Cn} - V_{2Cn})] \tag{7}$$

and

$$E_T = \frac{1}{2}P_t[(v_{1Ct} - v_{2Ct}) + (V_{1Ct} - V_{2Ct})] \tag{8}$$

The energy partitioning process leading to Eqs. 7 and 8, is intuitive, and does not follow directly from any principle of mechanics. If the partitioning were exact, the right hand side of Eq 7 would depend only on *e* thereby excluding any tangential effects and the right hand side of Eq 8 would depend only on μ thereby excluding any normal effects. However most collision reconstructions use the critical value of μ, $\mu = \mu_0$, which itself depends on the restitution *e* [1,7] so such an idealistic condition is not practical. To investigate these dependencies, the sensitivities of the equations to changes in the parameters is assessed with a numerical example.

Since there are two initially undeformed vehicle surfaces (one for each vehicle) and a single intervehicular crush surface, which depends on the collision geometry, the choice of the angle Γ can lead to some uncertainty in applications. The sensitivity of the partitioning to the choice of the value of Γ and to the amount of normal restitution (magnitude of *e*) are illustrated through the use of an example in which these factors are varied systematically. Another source of uncertainty that exists is the location of the impact center. This is not investigated here.

Prior to investigating the sensitivity of the energy partitioning, the influence of two parameters of the planar impact model on the apportionment of the energy is assessed. The particular parameters are the angle Γ and coefficient of restitution, *e*. The angle Γ defines the angular orientation of the *n-t* coordinate system relative to the *x-y* coordinate system as shown in Fig 2. Thus, the selection of Γ defines the direction along which the normal and tangential impulses act. Note that in the original CRASH3 method, visual estimation of the Principal Direction of Force (PDOF) was necessary. In the approach presented here, planar impact mechanics provides the PDOF as an output but the orientation of a single intervehicular crush surface must be estimated (through the choice of Γ).

This reconstruction approach starts with the measurement of the residual crush of the two vehicles involved in the collision. In general, the normal directions selected in the measurement process [9] for each of the vehicles are defined along the longitudinal and transverse coordinate axes of each individual vehicle. These normal directions are independent of the vehicle-to-vehicle collision geometry and are collinear only under certain circumstances such as head-on collisions. However, in the planar impact analysis, the relative angular orientation of the vehicles is established based on the combined damage profiles of the vehicles. The orientation of the vehicles first is established in an *x-y* scene coordinate system. An *n-t* coordinate system then establishes the angle Γ and a single intervehicular crush surface. Therefore, the angle Γ must in some way account for the two independent, vehicle-based normal directions from which the crush energies have been determined. The sensitivity of the energy apportionment of the planar impact mechanics model to changes in Γ is investigated using an example.

The other parameter of particular interest in the energy apportionment process is the coefficient of restitution, *e*. To a certain extent, the influence of *e* on the apportionment process depends on the selection of Γ, as the coefficient of restitution is defined using the preimpact and postimpact normal velocities at the impact center which in turn depend on Γ. Therefore it is expected that, although *e* varies typically between 0 and 0.3 for vehicular collisions [7], it will, in combination with Γ, influence the apportionment of the energy loss computed by planar impact mechanics along the normal and tangential directions. Note that under the assumption of the common velocity conditions [7], *e* = 0 and $\mu = \mu_0$, the energy loss is a maximum [16] and the velocities and energy loss determined by planar impact mechanics are independent of the selection of Γ. However, in applications where the energy determined from residual crush is used as part of a reconstruction, the selection of Γ plays a significant role in the apportionment of the work done by the normal and tangential impulses. It will be shown in a numerical example that the uncertainty is manageable.

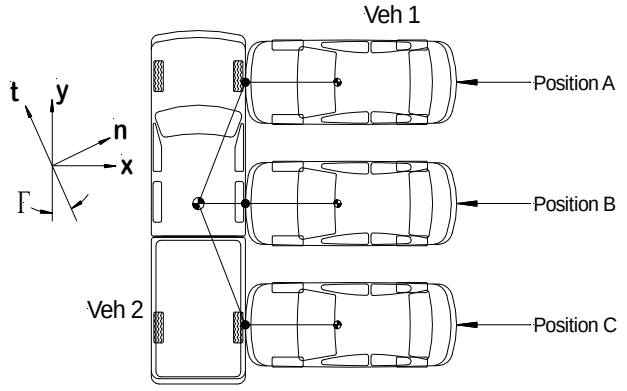

Figure 3. Positions and orientations of the vehicles used in the example.

The following example provides insight into the uncertainties and sensitivities of the reconstruction method and provides information useful to a

Table 1. Results from planar impact mechanics for changes in the initial speeds of the vehicles, the relative geometry at impact and *e* for all cases

v_{1x} mph	v_{2y} mph	e	μ_0	W_n ft-lb	W_t ft-lb	Position
-40	40	0.00	0.661	-30,097.2	-19,883.6	A
-40	40	0.15	0.594	-29,058.6	-20,308.8	A
-40	40	0.30	0.542	-26,793.1	-20,734.0	A
-40	40	0.00	0.369	-45,369.6	-16,747.6	B
-40	40	0.15	0.321	-44,348.8	-16,747.6	B
-40	40	0.30	0.284	-41,286.4	-16,747.6	B
-40	40	0.00	0.582	-24,427.5	-14,213.9	C
-40	40	0.15	0.484	-24,239.3	-13,788.6	C
-40	40	0.30	0.410	-22,824.4	-13,363.4	C
-20	40	0.00	1.121	-8,233.0	-18,466.1	A
-20	40	0.15	1.009	-7,867.0	-18,678.7	A
-20	40	0.30	0.919	-7,194.4	-18,891.4	A
-20	40	0.00	0.738	-11,342.4	-16,747.6	B
-20	40	0.15	0.642	-11,087.2	-16,747.6	B
-20	40	0.30	0.568	-10,321.6	-16,747.6	B
-20	40	0.00	1.448	-5,398.2	-15,631.3	C
-20	40	0.15	1.201	-5,457.4	-15,418.7	C
-20	40	0.30	1.022	-5,210.0	-15,206.1	C
-40	20	0.00	0.396	-28,679.8	-5,679.6	A
-40	20	0.15	0.360	-27,853.8	-5,892.2	A
-40	20	0.30	0.331	-25,800.9	-6,104.8	A
-40	20	0.00	0.185	-45,369.6	-4,186.9	B
-40	20	0.15	0.160	-44,348.8	-4,186.9	B
-40	20	0.30	0.142	-41,286.4	-4,186.9	B
-40	20	0.00	0.220	-25,844.9	-2,844.8	C
-40	20	0.15	0.176	-25,444.1	-2,632.1	C
-40	20	0.30	0.142	-23,816.5	-2,419.5	C

reconstructionist as a template for further, project specific analysis that considers additional collision geometries and combinations of parameters.

Example Consider the three different perpendicular collision geometries shown in Fig 3. The three relative positions of Vehicle 1 (Veh 1) to Vehicle 2 (Veh 2) are designated Position A, Position B, and Position C. The two vehicles shown are similar in geometry and inertial characteristics to a four door sedan (Veh 1) and pickup truck (Veh 2). Vehicle 1 has a curb weight of 2564 lb, a yaw moment of inertia of 1434.9 lbf-s^2-ft and an overall length of 14.6 feet. Vehicle 2 has a curb weight of 6345 lb, a yaw moment of inertia of 5192.4 lbf-s^2-ft and an overall length of about 21.8 feet. The center of mass of the pickup truck was moved rearward by about 2 feet to create symmetry for Positions A and C which simplifies the comparison of the results. These inertial parameters remain fixed throughout the example. The vehicles are given different initial velocities in the directions of their headings at the beginning of impact. The initial speeds of the vehicles are listed in Table 1. The coefficient of restitution, *e*, was varied in the analysis between 0 and 0.3 for each of the positions and all combinations of initial speeds of the vehicles. The angle Γ is zero for all cases listed in Table 1. (Variations in Γ are explored later.) Table 1 lists the apportionment of the work done by the normal and tangential impulses, W_n and W_t, given by Eqs. 7 and 8, respectively.

Examination of the results presented in Table 1 lead to the following observations about the nature of the impact between these two vehicles and the

apportionment of W_n and W_t for the corresponding range of parameters (for a constant Γ, collision geometry and critical impulse ratio).

■ For all the geometries, combinations of parameters and vehicle speeds, changes in the coefficient of restitution, e, leads to changes in both W_n and W_t.

■ With one exception, as e increases from 0 to 0.3, the amount of work done by the normal impulse decreases. The exception to this trend occurs for Veh 1 in Position C with the speed of Veh 1 at its slowest, v_1 = -20 mph, and the speed of Veh 2 at its fastest, v_2 = 40 mph. The largest percent change of W_n for a change in e is 12.6% for Position A.

■ The trend in the work done by the tangential impulse for constant Γ depends on the geometry of the vehicles at impact. For Veh 1 in Position A, the amount of work done by the tangential impulse increases as e increases. For Veh 1 in Position C, the amount of work done by the tangential impulse decreases as e increases. For Veh 1 in Position B, where the velocity of the mass center of Veh 1 passes through the center of mass of Veh 2, the amount of work done by the tangential impulse is independent of e. In general, the percent change of W_t is less than corresponding percent change in W_n for changes in e over the typical range for vehicular collisions. The largest percent change of W_t for a change in e is 15.0% for Position C with the speed of Veh 1 at its fastest, v_1 = -40 mph, and the speed of Veh 2 at it slowest, v_2 = 20 mph. This is the only case that was evaluated where the percent change of W_t is greater than the percent change of W_n.

■ The changes in initial speed of the vehicles for a given position of Veh 1 relative to Veh 2 lead to predictable trends in the apportionment of the normal and tangential work. For all three positions of Veh 1, an increase in the speed of Veh 1 for a fixed speed of Veh 2 leads to a increases in W_n with little or no change in W_t. Correspondingly, for all three positions of Veh 1, an increase in the speed of Veh 2 for a fixed speed of Veh 1 leads to increases in W_t with little or no change in W_n.

■ For the geometries and parameters investigated, large changes in e do not lead to large changes in μ_0. (Recall that a change in the coefficient of restitution changes the numerical value of the critical impulse ratio, μ_0.) For example, as e is changed from 0.15 to 0.3, a change of 100%, μ_0 changed from 0.594 to 0.542, a change of only about 9%. This satisfies intuition in that e is a parameter that is related to the normal direction and changes in its magnitude should ideally have little or no effect in the tangential direction.

■ Additional analysis for stationary Veh 2, v_2 = 0 mph, Γ = 0 and v_1 = -40 mph shows that the tangential impulse does no work for all three positions of Veh 1 shown in Fig 2. This trend is independent of e.

Table 2 Results from planar impact mechanics solution for changes in Γ, V_1 = -40 mph, V_2 = 40 mph, e = 0, Veh 1 in Position A

Γ deg	μ_0	W_n ft-lb	W_t ft-lb
-10	0.947	-21242.0	-28738.7
-5	0.794	-25,680.1	-24300.7
-4	0.766	-26569.5	-23411.1
-3	0.739	-27457.0	-22523.7
-2	0.712	-28341.5	-21631.2
-1	0.686	-29221.9	-20758.8
0	0.661	-30097.2	-19883.6
1	0.636	-30966.2	-19014.5
2	0.612	-31828.0	-18152.8
3	0.588	-32681.4	-17299.3
4	0.565	-33525.5	-16455.3
5	0.542	-34359.1	-15621.6
10	0.434	-38336.4	-11644.3

Having investigated some of the trends in the apportionment of W_n and W_t as the coefficient of restitution changes, the influence of Γ on these quantities is now analyzed. Using Veh 1 in Position A, the apportionment of W_n and W_t is evaluated for changes of Γ while the balance of the parameters remain fixed. The data shown in Table 2 lists the apportionment of W_n and W_t for the conditions listed.

Examination of the results presented in Table 2 lead to the following observations about the apportionment of W_n and W_t.

■ The data in Table 2 show the changes in W_n and W_t for one degree changes in Γ for $-5° \le \Gamma \le 5°$. Data at $\pm 10°$ are also included. These data are shown graphically in Figure 4 and the trends are essentially linear for this relatively narrow range of Γ. Small changes in Γ lead to small percentage changes in W_n and W_t for this example. Changes in Γ of 5° or more give rise to changes in W_n and W_t on the order of 10% to 20% from their nominal values for Γ = 0. This may seem large when considering the reconstruction of a collision. However, the uncertainty associated with the work and energy of the collision is tempered by the fact that the velocities (and the ΔVs) of the vehicles, typically the

desired output, are proportional to the square root of the energy loss (see Eq 2). This relationship reduces the uncertainty of the velocities of the vehicles as a function of changes in Γ.

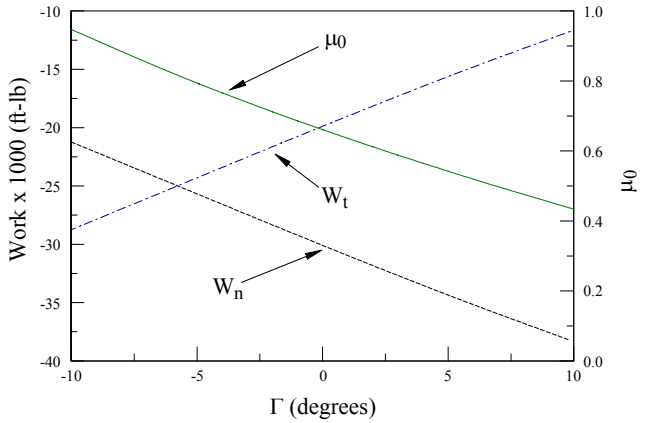

Figure 4. Plot of the data for W_n, W_t and μ_0 from Table 2; v_{1x} = -40 mph, v_{2y} = 40 mph, e = 0, Veh 1 in Position A.

■ As Γ changes from 0° to 180° the apportionment of the work done by the normal and tangential impulses changes in a cyclical fashion due to the trigonometric relationship between the quantities. The individual amounts of work done by the two impulses changes periodically but the total amount of energy lost in the collision (and hence the combined work done by the impulses) remains constant and is independent of Γ.

The range of parameters that were part of this example that investigated the sensitivity of the method is clearly not exhaustive. For instance, results for similar vehicle impact geometry but with Veh 1 as the heavier vehicle might show some different (and likely interesting) trends. Analysts using the method for the reconstruction of collisions that differ significantly from the example above may want to explore the range of uncertainty with parameters that more closely represent the collision of interest.

Guidelines for Use of the Method: The examples above provide insight into the apportionment of W_n and W_t for changes in several of the parameters. Several guidelines for the use of the reconstruction method can be assembled. These guidelines are directed primarily at the selection of the parameters and the manner in which to address uncertainty.

The choice of Γ affects the apportionment of W_n and W_t. Therefore, the user should examine uncertainty due to Γ. One way to select an initial value for Γ is to use the average angle of the two undeformed surfaces of the vehicles and their relative angular orientation at impact. Figure 5 shows two vehicles in their positions immediately after initial contact. The heading of Veh 1 relative to the x axis is 0° while the heading of Veh 2 is -135° (or +225°). This creates what is essentially a 45° angle between the undeformed front surfaces of the vehicles. Under these conditions the initial value for Γ should be half of that 45°, or 22.5° as indicated by the heavy line in Fig 5. The uncertainty for changes in Γ can be bracketed above and below using the angles associated with the two (undeformed) crush surfaces of the two vehicles involved. For the vehicles depicted in Fig 5, these angles would be Γ = 45° (Γ aligned with the front of Veh 2) and Γ = 0° (Γ aligned with the front of Veh 1). Note that the angles associated with this example are the extremes that the range of Γ can attain. If the vehicles in Fig 5 were closer to either a head-on or front-to-side collision, Γ would be bracketed to a narrower range. The two extremes, the head-on and the front-to-side collisions, the value of Γ becomes zero and the normal direction matches the normal directions selected during the residual crush measurement processes. The example above for a perpendicular collision geometry used Γ = 0 as the nominal value.

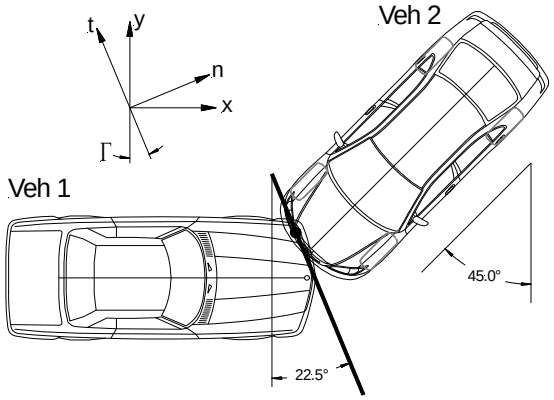

Figure 5. Geometry of vehicles showing the manner in which the nominal value of Γ is selected.

The selection of the coefficient of restitution differs little from the selection process for the application of the planar impact mechanics model without the consideration of the residual crush energy. Data exist [1, 6, 7, 17, 18] that present values of the coefficient of restitution determined from experimental collisions. The data suggest that the coefficient of restitution for most collisions involving light vehicles ranges between e = 0 and e = 0.3 with the majority of

the values likely at the lower end of that range.

In a reconstruction using an optimization algorithm to match the energy lost in the normal crush, the coefficient of restitution can be constrained during the optimization to vary between the bounds such as listed above. In this way, an additional degree of freedom is used in matching the energy loss objective. Inclusion of the (constrained) coefficient of restitution in the optimization scheme may provide additional insight into the solution reached. If, for example, the optimization algorithm consistently produces a value of *e* that is at the upper extreme of the constrained range, say $e = 0.3$ (or higher if the constraint is broadened) and there is little justification for *e* to take on these values (such as an impact at an axle) then a re-evaluation of other parameters, such as the geometry, may be in order.

In a similar manner the critical impulse ratio, μ_0, can be used to assess the nature of the collision. Values of the impulse ratio from experimental collisions [1, 6, 7] indicate that for the majority of collisions involving light vehicles, $\mu = \mu_0$; this indicates that relative tangential motion at the center of impact stops prior to separation. Unless the physical evidence strongly indicates otherwise, it is recommended that analyses of collisions using planar impact mechanics use $\mu = \mu_0$ (sideswipe collisions, where $\mu < \mu_0$ are the exceptions). The magnitude of the critical impulse ratio is dependent on initial conditions. The larger the initial relative tangential velocity at the impact center, the larger value of μ_0.

COMPARISON OF PLANAR IMPACT MECHANICS WITH BARRIER TEST DATA

Impulse from Load Cell Barrier Force v Time: In order to compare the impulse ratio computed from planar impact mechanics with its values measured from the crabbed vehicle tests conducted by Struble-Welsh Engineering, it was necessary to estimate values of the normal impulse and tangential impulses from the crabbed tests. As described earlier, the barrier used in the tests consisted of a main barrier face parallel to the crabbed vehicle's front bumper at initial contact, and a 24 inch "wing" barrier rigidly mounted perpendicular to the main barrier on the main barrier's down-field end.

The barrier wing was intended to load the vehicle front structure laterally while it was simultaneously undergoing frontal crush. This lateral loading also constrained the vehicle along the main barrier face, thereby forcing the barrier impulse ratio to equal the critical impulse ratio, μ_0, of planar impact mechanics. The critical impulse ratio can be calculated from impact velocity and restitution. It can therefore be calculated from impact conditions using planar impact mechanics and this value is compared to the impulse ratio estimated from test data, should the appropriate test data exist. In the crabbed test series, such data did indeed exist in the form of Force versus Time plots from the barrier load cells.

The barrier was divided into six banks of load cells: two on the left side of the main barrier, two on the right side of the main barrier, and two on the wing barrier. The two banks on the left side of the main barrier, top and bottom, were combined by the test facility into the plot SUM LEFT. The plots SUM RIGHT and SUM WING, for each test were similarly constrained. The plots are included in Appendix C.

The force versus time curves were digitized and numerically integrated for each test. In Table 3, the impulse values from each integration are reported in units of N-s. The Normal (total) is a sum of the left and right halves of the main barrier face. The Impulse Ratio is the Wing Impulse divided by the Normal Impulse.

The Impulse Ratio values calculated from test data and those from planar impact mechanics (see Appendix B, Table B1) from tests 1 and 2 show good agreement. The third test shows a dramatically higher value than from planar impact mechanics. Examination of the force versus time plots suggest a couple of reasons for this difference.

The first observation is that the main barrier pulse shape had a higher peak for each subsequent test,

Table 3. Impulse values, N-s, and impulse ratio values calculated from load-cell barrier data.

	Main Barrier			Wing Barrier	Impulse Ratio
Test	Left	Right	Normal		
1	2596	4612	7208	1720	0.239
2	3301	6788	10089	2857	0.283
3	3999	7715	11714	6262	0.535

particularly Test 3, while the wing barrier maintained more of a broad shape at max force. This may be due in part to the fact that the vehicle engaged the wing directly in the third test; the vehicle seemed to wrap itself around the wing. The very stiff right front suspension structure engaged the wing directly in this test, which it did not, or to a lesser extent, in the previous two tests. The very hard suspension engaging the relatively stiff wing may have created a fulcrum about which the vehicle rotated. This rotation about the wing end may have provided some relief at the left side of the front bumper, as this is the area that would initially rotate away from the barrier in this counter-clockwise rotation about the wing end. The rotation about the wing end would have the effect of extending the time duration of the vehicle interaction with the wing barrier (as compared to the main barrier interaction with the front bumper), extending the time duration of maximum force on the wing load cells.

Note the force value in the left side of the main barrier in Test 3 in Appendix C. While the right side and wing load cells again doubled their max force values from the previous test, the left side of the main barrier only increased by about 50%. This difference in the increase in force levels seen in the right side and wing load cells may also be related to the interaction described above.

It is also the case that while the wing barrier became more fully engaged in each subsequent test, such was not the case for the main barrier. As the vehicle sustained lateral crush in each test, the vehicle was foreshortened laterally, resulting in less overlap of the front of the vehicle onto the left side of the main barrier. This would also serve to decrease the amount of force, and impulse, recorded in the left side of the main barrier.

The crush energy analysis conducted on the data from these tests in [2] indicated that the vehicle frontal structure behaved in a constant force manner in this third test. This would suggest that the forces recorded in the main load cell barrier were less than they would have been had the vehicle front structure maintained a constant stiffness behavior. This mitigation of peak force in the frontal structure, as compared to the increasing lateral stiffness (and force) due to interaction with the very stiff right front suspension structure, would tend to affect the frontal (normal) impulse as compared to the lateral (tangential) impulse.

Finally, the right front structure had wrapped around the end of the wing barrier in the third test, engaging the end part of the wing parallel to the main barrier face. This surface of the barrier was not instrumented, and therefore any contribution of these forces to the total normal impulse was not included in the load cell data. This would serve to under-state the normal impulse and thereby contribute to an artificially high estimate of impulse ratio.

All of the above suggests that the characteristics of the pre-deformed vehicle in test 3, coupled with the dynamics of this third test (also influenced by the pre-deformed nature of the test vehicle), conspire to generate a somewhat high lateral impulse (as measured from load-cell data), along with a somewhat low normal impulse, resulting in the calculation of an artificially high impulse ratio as compared to what one would expect in a non-pre-crashed vehicle.

Restitution from Rigid Body Kinematics: It was of significant interest in this project to find a realistic estimate of the restitution values from the three tests. In this scenario the coefficient of restitution, which is defined as $e = -V_{Crn}/v_{Crn}$, pertains to the components of separation and impact velocity perpendicular to the main barrier face at a point on the contact surface at the front of the vehicle. The value of v_{Crn} is defined by the impact parameters and initial conditions, while the value of V_{Crn} must be measured from test data. Because any method chosen for finding V_{Crn} has some error associated with it, it was decided to use two different methods so that the results could be compared, and possibly averaged, to provide a reality check. The two methods used were rigid body kinematics and film analysis.

Rigid body kinematics provides the vector equation $\boldsymbol{V_P} = \boldsymbol{V_{cg}} + \boldsymbol{\omega} \times \boldsymbol{r_P}$. With this equation, the velocity, $\boldsymbol{V_P}$, of any point, P, on a rigid body may be found from the velocity at the center of mass, $\boldsymbol{V_{cg}}$, the body's rotational velocity, $\boldsymbol{\omega}$, and the position vector, $\boldsymbol{r_P}$, from the CG to the point P. Previous analysis [2] resulted in velocity at the center of mass (CG, in inertial coordinates) and angular velocity of the vehicle at separation. Separation was defined as the time at which rebound velocity reached its minimum. The only parameter here that still needed to be defined was $\boldsymbol{r}$, the position vector of the point of interest (in inertial coordinates). To determine $\boldsymbol{r}$, it is necessary to know where the point resided on the deformed vehicle, and how much the vehicle had rotated during the crush phase.

A full-scale deformation map was made of the vehicle after each test. On the full scale map, the

components of the vector ***r*** from the CG to the point at the center of the front edge of the bumper on the bent (post-test) vehicle were measured relative to the long axis of the undamaged vehicle.

To determine how much the vehicle had rotated from initial contact to separation, the average angular velocity during this phase was estimated to be half of the angular velocity at separation, and this average was applied over the contact duration to calculate an angular displacement at separation. Folding this angular displacement value into the components of ***r*** measured on the deformed vehicle resulted in the components of ***r*** in inertial coordinates. Then all the components necessary to perform the cross product and find the separation velocity at the point of interest were then available.

After performing the cross product and adding this velocity to $\boldsymbol{V}_{cg}$, the resulting separation velocity at the front of the vehicle was resolved into components perpendicular and parallel to the face of the main barrier. The component perpendicular to the main barrier prior to impact was then divided by the component of the impact velocity perpendicular to the main barrier and this was the restitution value reported in Table 4.

Restitution from Film Analysis of Experimental Barrier Collisions: Two overhead high-speed video cameras (1,000 fps) were included for each test, one wide angle and one narrow. The narrow angle camera showed approximately the front half the vehicle, and this was the view used for film analysis.

The point of interest near the front of the crushed vehicle was located for each test on the video and the perpendicular distance from that point to the barrier face was recorded at 10 ms intervals. This perpendicular position was plotted versus time. Rather than take the derivative of the line created by these points to find the velocity, the line was first smoothed with the Lowess and WLS smoothing routines of Axum software. Both smoothing routines were tried and the derivatives of the smoothed lines gave velocity values within 0.020 ft/s. The value of the velocity at the separation time value used in the rigid body kinematics analysis was then extracted from the data and divided by the component of impact velocity perpendicular to the barrier. These are the values of restitution shown in Table 4.

Table 4. Restitution values calculated from tests data using two different methods.

Test	Rigid Body Kinematics	Film Analysis	Avg
1	0.111	0.256	0.18
2	0.100	0.153	0.13
3	0.137	0.098	0.12

Because of the disparate methods used to determine *e*, the values for each test are quite different. Consequently, an average for each test is used in all following comparisons of the test data with results from planar impact mechanics.

Results from Planar Impact Mechanics: The crash tests consisted of three sequential crabbed rigid barrier tests (see Figure 1) of the same vehicle at successively higher speeds. An assumption is made that the relationship between the crush energy and the residual crush remains linear according to the CRASH3 model. This is illustrated in Fig 6 which shows that the crush energy for each test is an accumulation of the kinetic energy from test to test. This implies that an Energy Equivalent Speed, EES, [7, 19] exists for each test where, for *n* barrier tests,

$$EES = \sqrt{\sum_{i=1}^{n} v_{in}^2} \qquad (9)$$

and v_{in} is the initial normal velocity into the barrier. Regardless of any preexisting crush, each barrier test has a given initial speed, initial kinetic energy, coefficient of restitution, tangential coefficient, kinetic energy loss, ΔV, etc. Figure 7 is a plot of E^* (see Eq 3) as a function of residual crush, *C*, from the three successive barrier tests. It illustrates how the average measured crush using the NHTSA based crush stiffness coefficients [2] matches the linear CRASH3 model.

Two comparisons can be made for the test results for each barrier collision. One is a direct comparison of the experimental data of each crash with planar impact mechanics. Another is a comparison of the ΔV values calculated directly from CRASH3 with those of planar impact mechanics combined with CRASH3 crush energy that was described earlier. Appendix B contains two tables that summarize such comparisons.

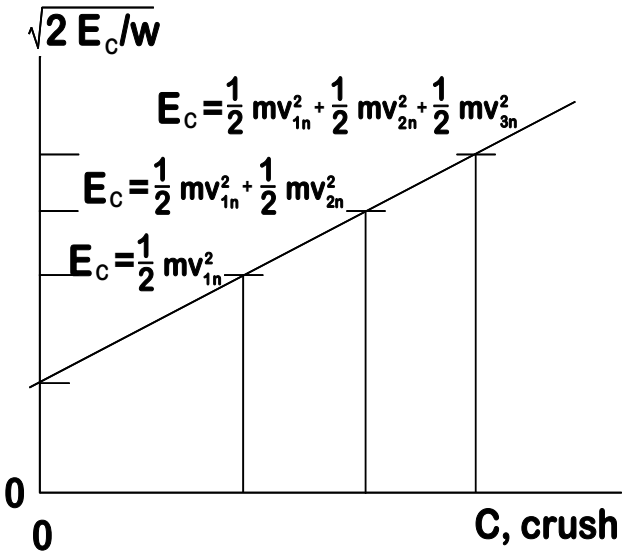

Figure 6. Linear CRASH3 model for sequential barrier crash tests of the same vehicle.

Comparison of Barrier Test Results with Planar Impact Mechanics: Table B1 gives direct comparison of calculated and measured barrier impact results. The ΔV values from the 3 collisions all are within 3%. The critical impulse ratios are of particular interest to the work in this paper. Table 3 lists the values determined from the experimental data. For the first collision (with an undamaged vehicle), the test value is $\mu_0 = 0.239$ and the computed value is $\mu_0 = 0.232$. For the second collision, the test value is $\mu_0 = 0.283$ and the computed value is $\mu_0 = 0.243$. The comparison is not as good for the third barrier collision; the test value is $\mu_0 = 0.535$ and the computed value is $\mu_0 = 0.245$. As already discussed above, the difference likely is due to existing vehicle damage making contact with the barrier wing in the third collision.

The comparison of the final angular velocities, Ω_1 and Ω_2, between test and computed values is illustrated. All of the values predicted by planar impact mechanics are higher than the test values, some by as much as a factor of 2. This is likely due to the winged geometry of the structure that may permit the development of a moment impulse [20] at the front of the vehicle which is ignored by this version of planar impact mechanics. This was not pursued in the study.

Comparison of CRASH3 Barrier Crush Energy with Planar Impact Mechanics Analysis: The crush energy and ΔV value based on the measured residual crush after each barrier test were computed using the CRASH3 damage algorithm using the crush stiffness coefficients from NHTSA tests [2]. These are corrected for tangential effects (using the PDOF from planar impact mechanics) and presented in Table B2, Appendix B. The crush energy loss for each test was equated to the work of the normal impulse as discussed above and also are presented in Table B2 (Appendix B). The main comparison is between the collision energy loss T_L predicted by CRASH3 and as predicted by planar impact mechanics and the corresponding values of ΔV. For Test 1, T_L = 11550 ft-lb (15.7 kJ) and ΔV = 9.9 mph (15.9 kph) from CRASH3. From planar impact mechanics, for Test 1, T_L = 12504 ft-lb (17.0 kJ) and ΔV = 12.2 mph (19.6 kph). The barrier test ΔV = 13.7 mph (22.0 kph). These comparisons and data from all three tests is presented in Table 5 using US units.

Tables 5 (US units) and 6 (Metric units) provide comparisons of crush energy and planar impact mechanics and crush energy with CRASH3 impact mechanics. (Note that in all applications of CRASH3 impact mechanics, the PDOF from planar impact mechanics was used, not a visually estimated value.)

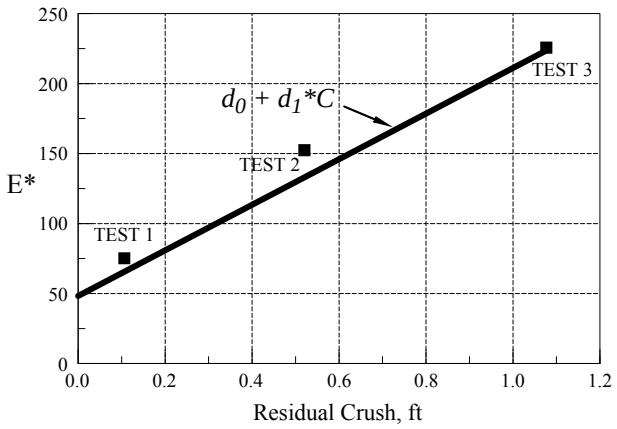

Figure 7. Comparison of residual crush energy of the sequential barrier tests with the linear CRASH3 model.

- For Tests 1 and 2, both the crush energy and ΔV values calculated using planar impact mechanics agree better with the measured values.
- For Test 3 (which had an adverse impact with the barrier wing), CRASH3 mechanics gives crush energy and ΔV values closer to the measured values.

DISCUSSION AND CONCLUSIONS:

Planar impact mechanics is a rigorous solution of the problem of the impact of two rigid bodies in a

plane. It should provide more accurate results than the point impact solution used by CRASH3 to calculate ΔV. In addition, the use of the work of the normal impulse to represent crush energy and the work of the tangential impulse to represent energy loss from tangential effects over the intervehicular contact surface eliminates the need for visual estimation of the PDOF and the use of the CRASH3 tangential correction factor.

In contrast to the common normal velocity condition of CRASH3, $e = 0$, the use of planar impact mechanics allows proper modeling of the effects of restitution. With this approach, it is unnecessary to make any corrections to the CRASH3 model to represent the effects of restitution. The use of planar impact mechanics and its critical impulse ratio allows a rigorous modeling of the tangential effects and automatically includes tangential energy loss without tangential correction. The use of the critical impulse ratio and planar impact mechanics for the purposes of reconstruction automatically takes into account the dependence of the tangential impulse on the initial conditions.

The use of planar impact mechanics (and the corresponding selection of a common crush surface) precludes the need for visual estimation of a PDOF, as required by CRASH3. With one exception (Test 3), comparison of constrained barrier tests shows that the critical impulse ratio computed by planar impact mechanics agrees well with experiments. This was also demonstrated by fitting of the RICSAC collision test data [21].

The selection of a common crush surface from observation and measurements of the actual damage leads to an estimation of the angle Γ. This process, which is based on physical measurements, should be more accurate than the estimation of the PDOF as required for application of CRASH3. A discussion of the how to select Γ and how this selection process can affect the uncertainty of a reconstruction was presented in the paper.

Table 5. Comparison of CRASH3, Planar Impact Mechanics and Test Values

	Test		CRASH3		Planar Impact Mechanics	
	Crush Energy	EES	Crush Energy	ΔV	Crush Energy	ΔV
Test	ft-lb	mph	ft-lb	mph	ft-lb	mph
1	13674	11.2	11550	9.9	12504	12.2
2	56876	22.8	47524	20.1	61334	23.6
3	125102	33.8	134329	33.8	145048	39.2

Table 6. Comparison of CRASH3, Planar Impact Mechanics and Test Values

	Test		CRASH3		Planar Impact Mechanics	
	Crush Energy	EES	Crush Energy	ΔV	Crush Energy	ΔV
Test	kJ	kph	kJ	kph	kJ	kph
1	18.6	18.0	15.6	15.9	17.0	19.6
2	77.2	36.7	64.5	32.4	83.3	37.9
3	170.0	54.3	182.4	54.3	197.0	63.1

APPENDIX A: Notation and Solution Equations of Planar Impact Mechanics

Notation, Subscripts:

cg	center of gravity
n, *t*	normal & tangential axes (Fig 2)
x, *y*	ground based axes (Fig 2)
r	relative
C	impact center
1, 2	vehicle number
P	point *P*

Notation, Variables:

C	crush
d_0, d_1	crush stiffness coefficients
d_a, d_b	distances, Appendix A
d_c, d_d	distances, Appendix A
d_e, d_e	distances, Appendix A
e	coefficient of restitution
E	energy
E^*	defined in Eq 3
E_C	energy loss due to crush
I	yaw moment of inertia
K_i	constants in Eq 4
m	mass
P	impulse
r	velocity ratio
T	kinetic energy
v	initial velocity
V	final velocity
W	work
ΔV	velocity change
Γ	crush surface angle
ω	initial angular velocity
Ω	final angular velocity
μ	impulse ratio

Summary of assumptions for planar impact mechanics:

1. A single dynamic contact, taking place over a short duration.
2. Forces other than the contact force and impulses of forces other than the contact force are negligible.
3. Rotational motion of the masses can be significant.
4. Initial velocities are known and final velocities are unknown.
5. Deformation is localized and small compared to the size of the bodies.
6. During the contact duration, position and orientation changes are negligibly small, velocity changes are instantaneous and accelerations are large.
7. The effects of the normal (crush) and tangential (sliding, shearing, entanglement, crush, etc.) contact processes are known (through coefficients).
8. A point (impact center), C, common to both vehicles and on the line of action of the contact impulse is known
9. A common crush plane defined by the angle Γ, is known.

Solution Equations of planar impact mechanics:

$$V_{1n} - v_{1n} = \bar{m}(1+e)v_{rn}q / m_1 \quad \text{(A1)}$$

$$V_{1t} - v_{1t} = \mu\bar{m}(1+e)v_{rn}q / m_1 \quad \text{(A2)}$$

$$V_{2n} - v_{2n} = -\bar{m}(1+e)v_{rn}q / m_2 \quad \text{(A3)}$$

$$V_{2t} - v_{2t} = -\mu\bar{m}(1+e)v_{rn}q / m_2 \quad \text{(A4)}$$

$$\Omega_1 - \omega_1 = \bar{m}(1+e)v_{rn}(d_c - \mu d_d)q / (m_1 k_1^2) \quad \text{(A5)}$$

$$\Omega_2 - \omega_2 = \bar{m}(1+e)v_{rn}(d_a - \mu d_b)q / (m_2 k_2^2) \quad \text{(A6)}$$

$$e = -V_{Crn} / v_{Crn} \tag{A7}$$

$$\mu = P_t / P_n \tag{A8}$$

$$I_1 = m_1 k_1^2 \tag{A9}$$

$$I_2 = m_2 k_2^2 \tag{A10}$$

$$v_{rn} = (v_{2n} - d_a \omega_2) - (v_{1n} - d_c \omega_1) \tag{A11}$$

$$V_{Crn} = V_{1n} + d_c \Omega_1 - V_{2n} + d_a \Omega_2 \tag{A12}$$

$$v_{Crn} = v_{1n} + d_c \omega_1 - v_{2n} + d_a \omega_2 \tag{A13}$$

$$\frac{1}{q} = 1 + \frac{\bar{m} d_a^2}{m_2 k_2^2} + \frac{\bar{m} d_c^2}{m_1 k_1^2} - \mu \left(\frac{\bar{m} d_c d_d}{m_1 k_1^2} + \frac{\bar{m} d_a d_b}{m_2 k_2^2} \right) \tag{A14}$$

$$d_a = d_2 \sin(\theta_2 + \varphi_2 - \Gamma) \tag{A15}$$

$$d_b = d_1 \sin(\theta_1 + \varphi_1 - \Gamma) \tag{A16}$$

$$d_c = d_1 \cos(\theta_1 + \varphi_1 - \Gamma) \tag{A17}$$

$$d_d = d_1 \cos(\theta_1 + \varphi_1 - \Gamma) \tag{A18}$$

$$d_e = d_c - \mu d_d \tag{A19}$$

$$d_f = d_a - \mu d_b \tag{A20}$$

$$r = \frac{(v_{2t} - d_b \omega_2) - (v_{1t} + d_d \omega_1)}{(v_{2n} - d_a \omega_2) - (v_{1n} + d_c \omega_1)} \tag{A21}$$

$$P_x = m_1 (V_{1x} - v_{1x}) \tag{A22}$$

$$P_y = m_1 (V_{1y} - v_{1y}) \tag{A23}$$

$$P_n = P_x \cos\Gamma + P_y \sin\Gamma \tag{A24}$$

$$P_t = -P_x \sin\Gamma + P_y \cos\Gamma \tag{A25}$$

$$\bar{m} = m_1 m_2 / (m_1 + m_2) \tag{A26}$$

$$\mu_0 = \frac{rA + (1+e)B}{(1+e)(1+C) + rB} \tag{A27}$$

$$A = 1 + \bar{m}(d_c^2 / I_1 + d_a^2 / I_2) \tag{A28}$$

$$B = \bar{m}(d_c d_d / I_1 + d_a d_b / I_2) \tag{A29}$$

$$C = \bar{m}(d_d^2 / I_1 + d_b^2 / I_2) \tag{A30}$$

APPENDIX B: Comparisons of Tests, CRASH3 and Planar Impact Mechanics

Table B1. Comparison of Barrier Tests With Planar Impact Mechanics
(comparisons are made both for $e = 0$ and for measured values of e)

	Struble			Welsh	Barrier	Tests			planar	impact	mechanics	analysis				
									Kinetic	Energy	Loss					
				Initial Kinetic					normal	tangent	total					
	v, ft/s	v_n ft/s	v_t ft/s	Energy, T_i ft-lb	e	$\|\mu\|$	Ω	ΔV, mph	T_{Ln}	T_{Lt}	T_L	$\|\mu\|$	Ω	ΔV, ft/s	ΔV, mph	PDOF
TEST1	19.23	16.6537	9.6150	18842.80	0.0000	-	-	-	14130.70	2236.90	16367.60	0.274	64.3	17.3	11.8	15.3
13.11 mph	19.23	16.6537	9.6150	18842.80	0.1800	0.239	37.7	13.7	13672.80	2236.90	15909.70	0.232	64.3	20.2	13.8	13.1
TEST2	33.91	29.3669	16.9550	58592.55	0.0000	-	-	-	43939.90	6955.70	50895.60	0.274	113.4	30.4	20.7	15.3
23.12 mph	33.91	29.3669	16.9550	58592.55	0.1300	0.283	53.8	24.0	49197.30	6955.70	50153.00	0.243	113.4	34.1	23.3	13.6
TEST3	42.56	36.8580	21.2800	92297.52	0.0000	-	-	-	69216.10	10956.90	80173.00	0.274	142.3	38.2	26.0	15.3
29.02 mph	42.56	36.8580	21.2800	92297.52	0.1200	0.535	69.3	29.8	68219.40	10956.90	79176.30	0.245	142.3	42.5	29.0	13.8

Table B2: Comparison of Tests, CRASH3 Analysis and Planar Impact Mechanics
(comparisons are made both for $e = 0$ and for measured values of e)

	Struble Welsh Engineering Tests										constant stiffness	CRASH3 $C_1,C_2,..,C_6$ reconstruction			planar impact $C_1,C_2,..,C_6$ mechanics reconstruction			
	initial	speed	ft/s	Initial Kinetic Energy, ft-lb			Crush Energy Ec	EES				Kinetic normal	Energy tangent	Loss, ft-lb total	Kinetic normal	Energy tangent	Loss, ft-lb total	
	v	vin	vit	T_I	e	$\|\mu\|$	$(1-e^2)mv_{1n}^2/2$	V_{BEQ}, ft/s	$\sqrt{2E_c/w}$	Cavg, ft	d0 + d1*C	T_{Ln}	$T_{Lt}=\tan^2\alpha$	T_L	T_{Ln}	T_{Lt}	T_L	$\|\mu\|$
TEST1	19.2	16.7	9.6	18843	0.00		14132	16.7	75.2	0.1062	65.56	10746	804	**11550**	10746	1701	12447	0.274
	19.2	16.7	9.6	18843	0.18	0.239	13674	16.4	74.0						10746	1758	**12504**	0.232
	13.1 mph																	
TEST2	33.9	29.4	17.0	58593	0.00		58077	33.8	152.4	0.5203	132.99	44215	3309	**47524**	44215	6999	51214	0.274
	33.9	29.4	17.0	58593	0.13	0.283	56876	33.4	150.8						44215	7120	**51334**	0.243
	23.1 mph																	
TEST3	42.6	36.9	21.3	92298	0.00		127300	50.0	225.7	1.0768	223.58	124976	9353	**134329**	124976	19784	144759	0.274
	42.6	36.9	21.3	92298	0.12	0.535	125102	49.5	223.7						124976	20073	**145048**	0.245
	29.0 mph																	

	e	CRASH3 $C_1,C_2,..,C_6$ reconstruction ΔV, ft/s	ΔV, mph	e	impact mechanics ΔV, ft/s	$C_1,C_2,..,C_6$ ΔV, mph
TEST 1	0.00	**14.5**	**9.9**	0.00	15.1	10.3
				0.18	**17.9**	**12.2**
TEST 2	0.00	**29.5**	**20.1**	0.00	30.5	20.8
				0.13	**34.5**	**23.6**
TEST 3	0.00	**49.5**	**33.8**	0.00	51.3	35.0
				0.12	**57.5**	**39.2**

APPENDIX C: Force v Time curves from load cell barrier data in SWE tests

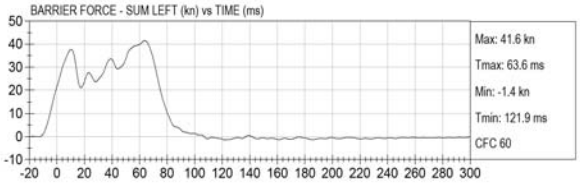

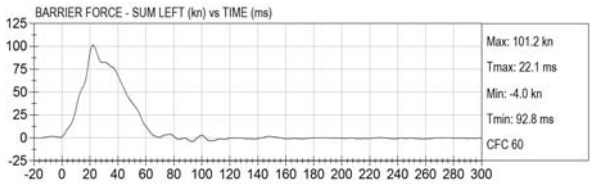

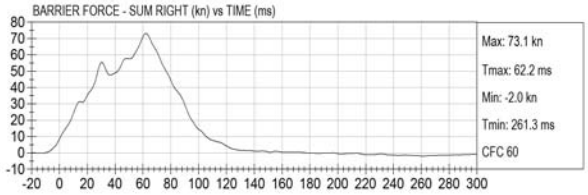

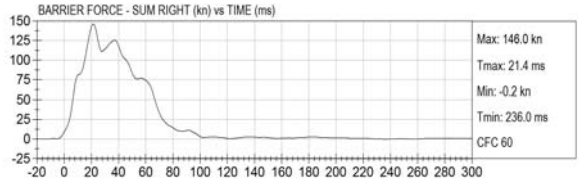

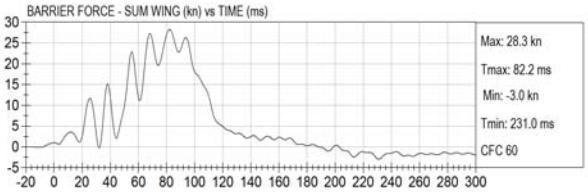

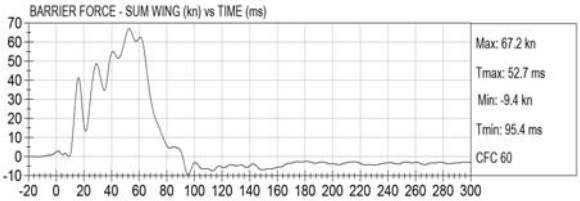

Test1 **Test 2**

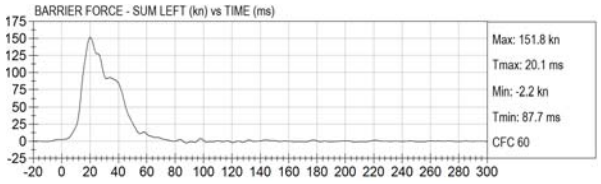

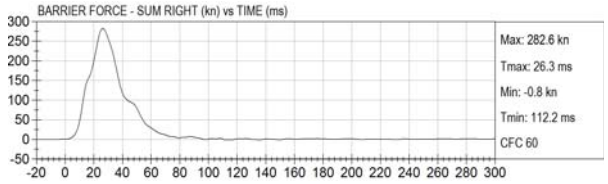

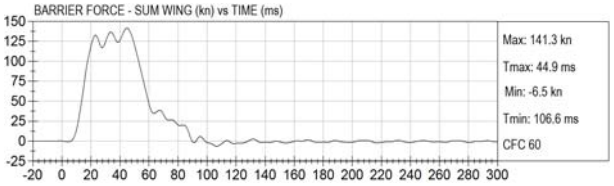

Test 3

References:

1. Brach, Raymond M. and R. Matthew Brach, "Crush Energy and Planar Impact Mechanics for Accident Reconstruction", Paper 980025, SAE, Warrendale, PA, 1998.

2. Welsh, K. J., D. E. Struble and J. D. Struble, "Lateral Structural Deformation in Frontal Impacts", Paper 2006-01-1395, SAE, Warrendale, PA, 2006.

3. Woolley, R, " The *IMPAC* Program for Collision Analysis", Paper 870046, SAE, Warrendale, PA, 1987.

4. Steffan, H. and A. Moser, "The Collision and Trajectory Models of PC-Crash", Paper 960886, SAE, Warrendale, PA, 1996.

5. Struble, D. E., "An Engineering Tool for Accident Reconstruction", Proceedings, *30th Annual Meeting of the American Association for Automotive Medicine*, Montreal, Quebec, 1986.

6. Brach, Raymond M., "Impact Analysis of Two-Vehicle Collisions", Paper 830468, SAE International Congress and Exposition, Detroit, MI, 1983.

7. Brach, Raymond M. and R. Matthew Brach, *Vehicle Accident Analysis and Reconstruction Methods*, SAE, Warrendale, PA, 2005.

8. Prasad, A."CRASH3 Damage Algorithm Reformulation for Front and Rear Collisions", Paper 900098, SAE, Warrendale, PA, 1998.

9. Smith, R. and N. Tumbas, "Measurement Protocol for Quantifying Vehicle Damage From An Energy Basis Point of View", Paper 880072, SAE, Warrendale, PA, 1988.

10. Campbell, K., "Energy as a Basis for Accident Severity", Paper 74056, SAE, Warrendale, PA, 1974.

11. McHenry, R. R., *CRASH3 User's Guide and Technical Manual*, NHTSA, DOT Report HS 805 732, February, 1981.

12. McHenry, B. and R. McHenry, "A Revised Damage Analysis Procedure for the Crash Computer Program ", Paper 861894, SAE, Warrendale, PA, 1986.

13, Rose, N., S. Fenton, R. Ziernicki, "Crush and Conservation of Energy Analysis: Toward a Consistent Methodology", Paper 2005-01-1200, SAE, Warrendale, PA, 2005.

14. Brach, Raymond M. and R. Matthew Brach, SAE Professional Development Seminar, *Vehicle Accident Reconstruction Methods*, SAE, Warrendale, PA, 2005.

15. Lord Kelvin and P. Tait, "Treatise on Natural Philosophy", Cambridge University Press, Cambridge, UK, 1903.

16. Brach, R., *Mechanical Impact Dynamics*, Wiley Interscience, New York, 1991.

17. Ishikawa, H. "Impact Model for Accident Reconstruction--Normal and Tangential Restitution Coefficients", Paper 930654, SAE, Warrendale, PA, 1993.

18. Germane, G. and K. Monson, "Determination and Mechanisms of Motor Vehicle Structural Restitution for Crash Test Data", Paper 1999-01-0097, SAE, Warrendale, PA, 1999.

19. Kerkhoff, J., S. E. Husher, M. S. Varat, A. M. Busenga and K. Hamilton, "An Investigation Into Vehicle Frontal Impact Stiffness, BEV and Repeated Testing for Reconstruction", Paper 930899, SAE, Warrendale, PA, 1993.

20. Brach, R. M., "An Impact Moment Coefficient for Vehicle Collision Analysis", Paper 770014, Transactions, SAE, Warrendale, PA, 1977.

21. Brach, R. M. "Identification of Vehicle and Collision Impact Parameters from Crash Tests", Paper 83-DET-13, ASME Design Technical Conference, Dearborn, MI, 1983.